Atomic Interferometry Using Stimulated Raman Transitions

Mark Kasevich and Steven Chu

Departments of Physics and Applied Physics, Stanford University, Stanford, California 94305
(Received 23 April 1991)

The mechanical effects of stimulated Raman transitions on atoms have been used to demonstrate a matter-wave interferometer with laser-cooled sodium atoms. Interference has been observed for wave packets that have been separated by as much as 2.4 mm. Using the interferometer as an inertial sensor, the acceleration of a sodium atom due to gravity has been measured with a resolution of 3×10^{-6} after 1000 sec of integration time.

The potential utility of atom interferometers has been previously discussed [1,2]. As sensitive accelerometers they can be used for a variety of precision measurements such as a search for a net charge on atoms, fifth-force experiments, and tests of the equivalence principle and general relativity. Atom interferometers can also be used in Berry's phase measurements or in studies of the Aharonov-Casher effect [3]. Finally, since atom interferometers are also sensitive to the atom's internal degrees of freedom, experiments not accessible to neutron or electron interferometry are possible.

Atomic diffraction from microfabricated matter gratings [1] and from intense standing waves of light [4] have been experimentally demonstrated, and discussed as a potential means of coherently splitting an atomic wave function. It has also been suggested that the photon recoil acquired by an atom when making an optical transition be used as an atomic beam splitter [5]. More recently, an atom interferometer in a Young's double-slit diffraction geometry has been demonstrated [6].

In this Letter we describe an atom interferometer where the atomic wave function of a sodium atom is coherently split by a two-photon Raman transition between the $F = 1$, $m_F = 0$ and $F = 2$, $m_F = 0$ ground states (hyperfine splitting = 1.77 GHz) of the atom. With the laser beams tuned near the $3S_{1/2}$-$3P_{3/2}$ sodium transition, we have previously demonstrated mechanical effects of this two-photon transition: If the two laser beams are counterpropagating, atoms making the Raman transition will experience a velocity recoil $v_r = 2\hbar k/M \approx 6$ cm/sec [7]. With laser-cooled atoms in an atomic fountain [8], transit times through the apparatus can approach 0.5 sec, yielding separations on the order of 1 cm.

Our interferometer separates and recombines an atom by using a $\pi/2$-π-$\pi/2$ sequence of Raman pulses. The use of NMR concepts [9] is appropriate for our situation, and if the laser detunings from either of the hyperfine ground states to the excited $3P_{3/2}$ state are large compared to the Rabi frequencies of the laser beams and the linewidth of the $3P_{3/2}$ state, the three-level system discussed here can be reduced to an equivalent two-level system [10]. First consider a wave packet with mean momentum p (p is the momentum component along the direction of the laser beams) and internal state $|1\rangle$. The first $\pi/2$ pulse puts the original state $|1,p\rangle$ into a superposition of states $|1,p\rangle$

and $|2,p+2\hbar k\rangle$. After a time Δt, the wave packets will have separated by an amount $2\hbar k \Delta t/M$. The π pulse then induces the transitions $|1,p\rangle \rightarrow |2,p+2\hbar k\rangle$ and $|2,p+2\hbar k\rangle \rightarrow |1,p\rangle$, and after another interval Δt, the two wave packets merge again. By adjusting the phase of the final $\pi/2$ pulse, the atom can be put into either of the hyperfine states. If the laser beams are aligned to be perpendicular to the motion of the atoms, we have the atomic analog to an optical Mach-Zehnder interferometer as shown in Fig. 1(a). Figure 1(b) illustrates a configuration where the atomic separation is along the direction of motion. We used this form of the interferometer to measure the acceleration of an atom due to gravity.

The final state of the atom depends on the phase difference between the two paths $1 \rightarrow 2 \rightarrow 4$ and $1 \rightarrow 3 \rightarrow 4$ of Fig. 1 during the free evolution of the atom, and the phase of the atom relative to the phases of the optical driving fields. Under conditions where the action $S = \int_\Gamma L \, dt$ (L is the Lagrangian of the atom) is much larger than $\hbar$, the free-evolution contribution to the phase of the atom reduces to $\phi_f = \int_\Gamma (\mathbf{k}_a \cdot d\mathbf{x} - \omega_a \, dt)$, where $\mathbf{p}_a = \hbar \mathbf{k}_a$ and $E_a = \hbar \omega_a$ are the classical momentum and total energy of the atom, respectively, along the classical path Γ [11]. For the interferometers described here, the phase difference between the two paths is zero for an atom in a constant gravitational field. This is to be contrasted with neutron interferometers where the interaction with the beam splitter does not change the neutron's energy so the phase difference from the $\int \omega \, dt$ term is zero, but the $\int \mathbf{k} \cdot d\mathbf{x}$ term gives a nonzero contribution [12].

The phase shifts arising from the atom's interaction with the light do not vanish. The net phase shift between the two paths can be written in the form $\Delta \phi_l = \phi_1 - \phi_2 - \phi_3 + \phi_4$ (see Fig. 1), where $\phi_i = \mathbf{k}_l \cdot \mathbf{x}_i - \omega_i t_i$ in the limit where effects due to the finite duration of the pulse can be ignored [13]. In this expression, $\mathbf{k}_l = \mathbf{k}_1 - \mathbf{k}_2$ is the difference of the photon wave vectors, $\mathbf{x}_i$ the position of the atom, t_i the time the light is pulsed on, and ω_i the rf frequency for that pulse. Note that the $\pi/2$-π-$\pi/2$ pulse sequence ensures that the net phase shift from the $\mathbf{k}_l \cdot \mathbf{x}_i$ term is velocity independent so that the fringe contrast can be preserved in the presence of an inhomogeneous velocity distribution.

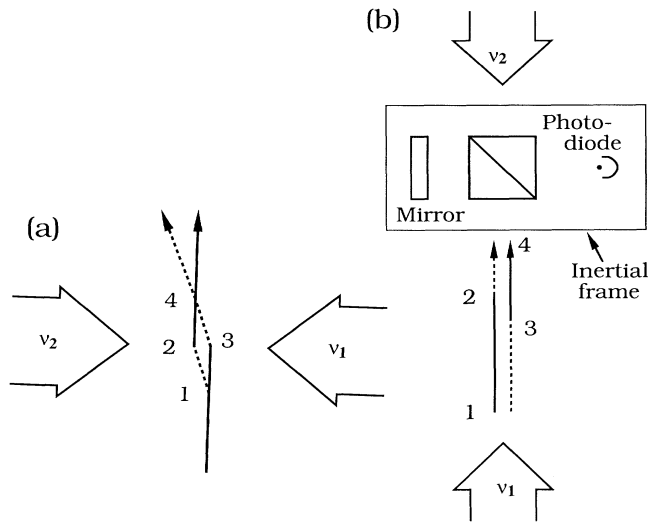Phase shifts due to the $\omega_i t_i$ term depend on ω_i for the

FIG. 1. Diagrams of the $\pi/2$-π-$\pi/2$ pulse interferometer described in the text. The mechanical recoil from the first $\pi/2$ pulse coherently splits (position 1) the atomic wave packet. A π pulse (positions 2 and 3) redirects each wave packet's trajectory. By adjusting the phase of the second $\pi/2$ pulse (position 4), the atom can be put into either $|1\rangle$ or $|2\rangle$. (a) The atom's mean velocity is orthogonal to the laser beams. (b) The case where the atom is traveling parallel to the beams (overlapping wave-packet trajectories are slightly displaced). The inertial frame, consisting of a beam splitter, mirror, and photodiode, is suspended just above the vacuum can. In our experiment, the atom is prepared in the $|1\rangle$ state (solid lines) and detected in the $|2\rangle$ state (dashed lines).
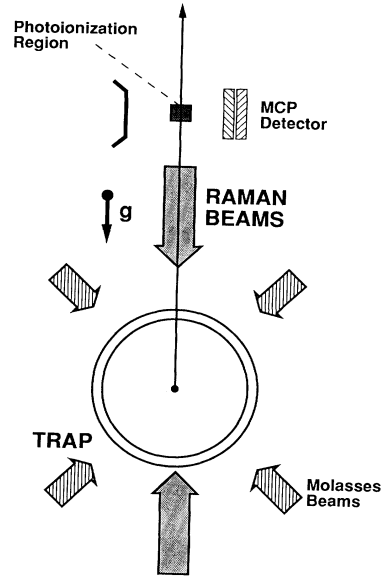
FIG. 2. A schematic of the apparatus used to demonstrate the interferometer illustrated in Fig. 1(b). Atoms were loaded into an optomagnetic trap, cooled, launched, and then optically pumped into the $F=1$ hyperfine state. Approximately 50 msec following their launch, the set of Raman beams is pulsed on three times to drive $\pi/2$-π-$\pi/2$ pulse sequence. After 135 msec, atoms in the $F=2$ state were detected by resonant photoionization. The repetition rate of the experiment was 1 Hz. Not shown are the other set of molasses beams and the atomic beam used to load the trap.

three pulses. If $\omega_i = \omega_0$ for all pulses, one can show that $\Delta\phi_l = -\mathbf{k}_l \cdot \mathbf{g}(\Delta t)^2$, where Δt is the time between pulses. This result is equivalent to an expression derived by Bordé [5]. For large accelerations and/or long measurement times Δt, it is convenient to change ω_i to keep in resonance with the atoms. (The $\pi/2$ pulse must remain a $\pi/2$ pulse as the atom accelerates.) If the frequency difference of the light is chirped to stay in resonance with the atom as it accelerates, the net phase shift is again zero. If, instead, the three frequencies of the light pulses [14] are fixed at $\omega_1 = \omega_0$, $\omega_{2,3} = \omega_0 + \omega_m$, $\omega_4 = \omega_0 + 2\omega_m$, where $\omega_m \sim \mathbf{k}_l \cdot \mathbf{g}\Delta t$, then $\Delta\phi_l = -\mathbf{k}_l \cdot \mathbf{g}(\Delta t)^2 + 2\omega_m\Delta t$.

The experimental apparatus (see Fig. 2) has been described in prior publications [7,8]. Briefly, $\sim 10^7$ atoms were loaded into an optomagnetic trap [15] from a slowed Na beam. The atomic beam was slowed by a counterpropagating, frequency-chirped laser. After 0.8 sec the magnetic field used to trap the atoms was shut off, and the atoms were further cooled in polarization-gradient optical molasses [16] to a temperature of ~ 30 μK. 500 μsec after the magnetic field was shut off, the ~ 4-mm-diam ball of atoms was launched vertically in a moving molasses light field by shifting the frequencies of

the molasses beams with vertical components by ± 2.9 MHz [7]. The atoms were then optically pumped into the $F=1$ hyperfine state.

The two Raman laser beams were derived from a second dye laser tuned ~ 2.5 GHz below the $F=2 \rightarrow 3$ resonance. One beam was passed twice through a ~ 30-MHz acousto-optic modulator while the other passed through a ~ 1.71-GHz electro-optic modulator. Line broadening of the transition due to mirror vibrations was eliminated with a fast servo system that monitored and corrected the beat note of the two laser beams just outside the vacuum can [see Fig. 1(b)]. A beam splitter and mirror used to overlap the two laser beams were mounted on an interferometrically stable inertial reference frame (a ~ 35-kg brass plate suspended from the ceiling by surgical tubing), and the measured beat note was phase locked to a stable rf reference by changing the frequency of the ~ 30-MHz modulator. A random shift in the position of the platform during the course of the scan by $\sim \lambda/4$ in the measurement time would destroy fringe contrast. For each Raman pulse, light at ν_L and $\nu_L - (60$ MHz) (where ν_L is the laser carrier frequency) was first turned on for 40 μsec to let the servo system phase lock to the beat note. The rf sideband from the electro-optic modulator at 1.71 GHz was then pulsed on for the time required to drive the $\pi/2$ or π pulse.

Before entering the vacuum can, the Raman beams were expanded to an ~ 2-cm $1/e^2$ diameter. Wave-front curvature was measured interferometrically to better than $\lambda/10$ in the central 0.5 cm of each beam. The vacuum-can windows were measured to be flat to at least the same degree over this area. The beams were centered on the trapping region and parallel to **g** to better than 2 mrad.

The three rf frequencies for the $\pi/2$, π, and $\pi/2$ Raman pulses were generated by mixing one of three ~ 60-MHz synthesizers with the 1.64-GHz output of an HP8665A synthesizer. The 1.64-GHz carrier and 1.58-GHz sideband were removed with an rf filter, leaving only the 1.71-GHz sideband to drive the electro-optic modulator. All synthesizers were referenced to timing signals from a SRS FS700 LORAN-C receiver which has a short-term stability of 1 part in 10^{-11}. The relative phases of the low-frequency synthesizers were synchronized by adjusting the phase of one of the oscillators so that the initial phase difference $\Delta\phi^0 = \phi_1^0 - 2\phi_2^0 + \phi_3^0$ was constant, where $\phi_i(t) = \omega_i t + \phi_i^0$ is the phase of the ith oscillator. Phase noise of one of the low-frequency oscillators produced a $20°$ uncertainty in $\Delta\phi^0$.

The interferometer signal was derived from the measurement of the Raman transition from the $F=1$, $m_F=0$ state to the $F=2$, $m_F=0$ state. Atoms excited into the $F=2$ state were resonantly ionized and the ions were detected by a microchannel plate as shown in Fig. 2. A bias magnetic field of ~ 85 mG was applied along the propagation axis of the light to remove the degeneracy between field-sensitive $m_f = \pm 1 \rightarrow \pm 1$ transitions and the field-insensitive $m_f = 0 \rightarrow 0$ transition. Since the ~ 600-kHz Doppler width of the atomic fountain (due to a spread $\Delta v_{\text{fountain}} \simeq 20$ cm/sec) was much larger than the ~ 120-kHz splitting between the field-sensitive and field-insensitive transitions, the field-sensitive transitions were also excited by the $\pi/2$ and π pulses. Atoms making the field-insensitive transition were distinguished from those in the field-sensitive state by their time of flight to the

detection region. A horizontally propagating 15-nsec pulse of 355-nm light apertured to a 4 mm (vertical)$\times 8$ mm (horizontal) rectangle intersected a vertically propagating 1-μsec pulse of light resonant with the $F=2 \rightarrow 3$ transition. The resonant beam ($1/e^2$ diameter$\simeq 5$ mm) copropagating with one of the Raman beams created an approximately cylindrical detection region that ionized only those atoms whose trajectories were near the center of the Raman beams.

Figure 3 shows a scan of $\omega_m/2\pi$ versus ionization signal for the $\pi/2$-π-$\pi/2$ sequence. The pulses were separated by 10 msec, and the time required to drive a π pulse was 65 μsec with a 2.5-GHz detuning of the carrier from the optical resonance. The polarizations of the Raman beams were crossed linear. Each data point represents 40 fountain launches at a rate of 1 launch/sec. The 25-Hz linewidth corresponds to a Doppler resolutions $\Delta v/c = \Delta v/(v_1 + v_2)$ of 7.5 μm/sec.

The fringe contrast would be 100% if the pulse length δt of the Raman $\pi/2$ and π pulses were sufficiently short to address all of the atoms in the velocity distribution of the atomic fountain, i.e., if $(1/\delta t)/(v_1 + v_2) \gg \Delta v_{\text{fountain}}/c$. For the conditions in Fig. 3, the expected fringe contrast was decreased to 27% because some of the atoms in the velocity distribution were partially out of resonance with the driving laser pulses. Consequently, these atoms were excited but did not see the full $\pi/2$ and π pulses. The expected fringe contrast after background subtraction was observed for 1-ms delay times between pulses as shown in Fig. 4(a). However, the fringe contrast in Fig. 3 is 12% and a "best run" with a 40-msec delay between pulses gave a 7% contrast [Fig. 4(b)]. We suspect movement of the reference "inertial" frame and wave-front instabilities in the Raman beams to be the dominant sources of the loss of contrast at the longer delay times. With improved engineering, we believe that it should be possible to ap-
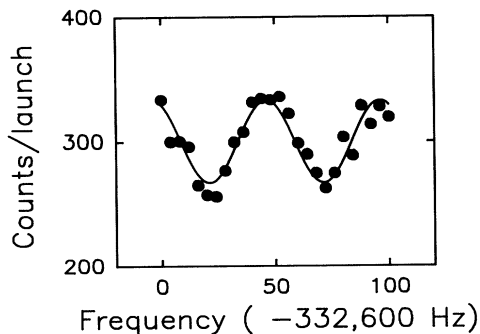

FIG. 3. Interferometer fringes from a frequency scan of the Raman laser beams when the time between pulses is 10 msec. The solid line is a nonlinear least-squares fit to the data. The linewidth of the resonance is determined by the time between the $\pi/2$ and π pulses, and is not a free parameter.
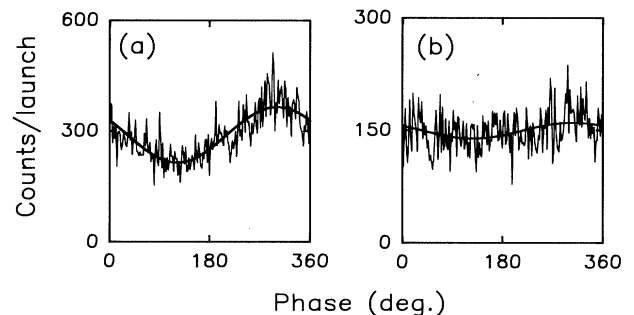

FIG. 4. Interference fringes for (a) $\Delta t = 1$ msec and (b) $\Delta t = 40$ msec pulse delay times. Phase is scanned by shifting the phase of the rf sideband used for the final $\pi/2$ pulse by the indicated amount. The heavy lines are nonlinear least-squares fits of sine functions to the data. In the case of the 40-msec delay time, the maximum wave-packet separation is 2.4 mm, and the velocity fringes have a width of 1.8 μm/sec.

proach 100% fringe contrast for measurement times on the order of $\Delta t = 0.1$ sec.

A least-squares fit with a sine function could determine the center of the fringe in Fig. 3 to ± 0.6 Hz. The fitted uncertainty yields a sensitivity to changes in g at the level of 3×10^{-6} after an integration time of 1000 sec for all the data shown in Fig. 3. The data in Fig. 4(b) have an inherent resolution of 6×10^{-7} uncertainty. The resolution was limited by the loss in interferometer contrast, a background counting rate, and fluctuations in the signal rate. The background counts were due to population of the $F = 2$ state from spontaneous emission from the $3P_{3/2}$ state and they occurred at 20% of the peak signal rate. Sources of noise included the $\sim 10\%$ intensity fluctuations in the Nd-doped yttrium-aluminum-garnet laser, $\sim 25\%$ fluctuation in the number of trapped atoms, random phase shifts induced by motion of the inertial reference frame, and pointing instabilities in the laser used to generate the Raman beams.

An absolute measure of g can, in principle, be determined with great accuracy. Systematic phase shifts associated with magnetic-field inhomogeneities in the present apparatus were at the ~ 1-Hz level given the 8-mG field gradient in the interaction region (measured by aligning the Raman beams to be copropagating and tuning across the field-sensitive transitions). A deviation from vertical of the Raman beams by 2 mrad (the upper limit on the alignment of the beams with the local vertical) will create a systematic shift in g at the level of 2×10^{-6}. Since these systematic errors decrease quadratically with the perturbing influence, we believe that an absolute measurement of g on an atom can ultimately be done with an uncertainty better than 1 part in 10^{-10}, and relative measurements should be possible with orders of magnitude greater precision. With changes in the experimental arrangement, $\hbar/M$ can also be determined with great accuracy through a precision measurement of the recoil velocity.

We have also operated the interferometer in the Mach-Zehnder configuration. Working with 2-cm-diam laser beams, atoms with an upward velocity of 250 cm/sec were separated by 72 μm using a 1.2-msec delay between pulses. By working at the peak of a ballistic trajectory, a delay time of ~ 0.2 sec is possible, giving a wave-packet separation of 6 mm. In this geometry, it should be possible to spatially resolve the arms of the interferometer.

The precision of this type of atom interferometer follows directly from the high-frequency resolution made accessible with atomic fountains [8], and the use of optical transitions between ground states of an atom, which allows radio-frequency stability of the excitation with a Doppler sensitivity in the ultraviolet frequency range [7]. We plan to use this type of interferometer to improve the tests of the charge neutrality of atoms, tests of the equivalence principle, and for searches of gravitational anomalies.

[1] D. W. Keith, M. L. Schattenburg, Henry I. Smith, and D. E. Pritchard, Phys. Rev. Lett. **61**, 1580 (1988).

[2] J. F. Clauser, Physica (Amsterdam) **151B**, 262 (1988).

[3] R. Hagen, Phys. Rev. Lett. **64**, 2347 (1990).

[4] P. L. Gould, G. A. Ruff, and D. E. Pritchard, Phys. Rev. Lett. **56**, 827 (1986).

[5] C. J. Bordé, Phys. Lett. A **140**, 10 (1989). In this paper, Bordé points out that wave-packet interference may have been inadvertently demonstrated in experiments using Ramsey fringes in the optical domain.

[6] O. Carnal and J. Mlynek, Phys. Rev. Lett. **66**, 2689 (1991).

[7] M. Kasevich, D. S. Weiss, E. Riis, K. Moler, S. Kasapi, and S. Chu, Phys. Rev. Lett. **66**, 2297 (1991).

[8] M. Kasevich, E. Riis, S. Chu, and R. G. DeVoe, Phys. Rev. Lett. **63**, 612 (1989).

[9] See, for example, L. Allen and J. H. Eberly, *Optical Resonance and Two-Level Atoms* (Wiley, New York, 1975).

[10] See, for example, R. G. Brewer and E. L. Hahn, Phys. Rev. A **11**, 1641 (1975).

[11] R. P. Feynman and A. R. Hibbs, *Quantum Mechanics and Path Integrals* (McGraw-Hill, New York, 1965).

[12] D. M. Greenberger and A. W. Overhauser, Rev. Mod. Phys. **51**, 43 (1979).

[13] The expression for $\Delta\phi$ follows from Eq. (V.26) of N. Ramsey, *Molecular Beams* (Oxford Univ. Press, London, 1956), p. 127.

[14] Most frequency synthesizers are not sufficiently phase stable during a phase continuous frequency sweep to take advantage of the inherent precision in atom interferometry.

[15] E. L. Raab, M. Prentiss, A. Cable, S. Chu, and D. E. Pritchard, Phys. Rev. Lett. **59**, 2631 (1987).

[16] J. Dalibard and C. Cohen-Tannoudji, J. Opt. Soc. Am. B **6**, 2023 (1989); P. J. Ungar, D. S. Weiss, E. Riis, and S. Chu, J. Opt. Soc. Am. B **6**, 2058 (1989).